

J. Synchrotron Rad. (1999). **6**, 776–778

Spatial cross-over of polarons across the CMR transition in $\text{La}_{0.75}\text{Ca}_{0.25}\text{MnO}_3$ system

A.Lanzara^a, F.Natali^a, N.L.Saini^a,
A.Bianconi^a, and P.G.Radaelli^b

^aUnità INFM and Dipartimento di Fisica, Università di Roma "La Sapienza", 00185 Roma, Italy, ^bRutherford Apleton Laboratory (RAL), Chilton, Didcot, OX11 0QX, UK. E-mail: lanzara@roma1.infn.it

We have measured high resolution Mn K-edge x-ray absorption near edge structure (XANES) and extended x-ray absorption fine structure (EXAFS) to investigate the local atomic displacements in the MnO_6 octahedra and their importance to the colossal magnetoresistance in the $\text{La}_{0.75}\text{Ca}_{0.25}\text{MnO}_3$ system. A combined analysis of the XANES and EXAFS shows that the colossal-magneto resistance (CMR) transition is characterized by a transition from a phase of delocalized intermediate polarons to a phase showing coexistence of the intermediate and small polarons accompanied by the opening of a gap at E_F due to Jahn Teller splitting of e_g orbitals.

Key words: polarons, manganites, CMR, metal-insulator transition.

1. Introduction

Strong correlation of lattice with charge and spin structure in manganese perovskites has been a point of wide interest during recent years (Rao et al, 1998) as these materials are suitable model compounds for further understanding of the strong electronic correlations in the solid state physics.

Among manganese oxide systems, the $\text{La}_{1-x}\text{Ca}_x\text{MnO}_3$ family shows complex but fascinating phase diagram (Schiffer et al, 1995) with doping and temperature. At $T=0$ K at low doping, for $x<0.15$, it shows an antiferromagnetic phase, for $0.15<x<0.5$ a ferromagnetic metallic phase and a charge ordered phases for $x\geq 0.5$. In the ferromagnetic doping regime, the system shows a colossal magneto resistance (CMR) and turns into a paramagnetic insulator above a critical temperature T_C . It has been observed that the CMR transition is accompanied by an elongation of the Mn-O bondlengths of the MnO_6 octahedra suggesting that the atomic distribution around the Mn site plays important role in the metal-insulator and magnetic transition at T_C . It is now getting established that the metal-insulator transition in the manganites is a polaronic transition (Zhao et al, 1996, Bishop et al, 1997, Goodenough & Zhou, 1997; Millis, 1998). In fact, a transition from intermediate to small polarons in the region around T_C has been indicated by an anomalous temperature dependence of Debye Waller factors and lattice parameters (Radaelli et al, 1996), the local pair distribution function, derived by neutron powder diffraction (Egami et al, 1997; Billinge et al, 1996) and several other studies (De Teresa et al, 1997). The Mn K-edge extended x-ray absorption fine structure (EXAFS) studies have also given similar indications (Tyson et al, 1996; Booth et al, 1997). Recently we have characterized (Lanzara et al, 1998) the local polaronic distortions of the MnO_6 octahedra in a representative system by Mn K-edge EXAFS

exploiting high intensity of ESRF and fluorescence detection mode. The results on the $\text{La}_{0.75}\text{Ca}_{0.25}\text{MnO}_3$ (LCMO) compound shows that the CMR transition is related to the spatial extension of the polaronic charge in the manganites in which the metallic phase ($T<T_C$) is characterized by intermediate polarons, having small local lattice distortions, while the insulating phase ($T>T_C$) is characterized by a coexistence of small polarons, having large local lattice distortions, and the intermediate polarons.

In this communication, we report further evidence by a combined analysis of the Mn K-edge x-ray near edge structure (XANES) and EXAFS on the LCMO system. Using fluorescence detection mode we were able to isolate partial absorption cross section only due to Mn 1s initial state from x-ray absorption due to other atomic species in the system. The approach, combined with high energy resolution has allowed us to follow the temperature dependence of the selected core transitions to unoccupied states at the Fermi level, $1s \rightarrow e_g$, across the CMR transition in the LCMO system.

2. Experimental

A powder sample (Radaelli et al, 1996) of $\text{La}_{0.75}\text{Ca}_{0.25}\text{MnO}_3$ ($T_C=240\text{K}$) was used for the Mn K-edge x-ray absorption measurements at the beam-line BM29 of European Synchrotron Radiation Facility (ESRF) at Grenoble. The high resolution x-ray absorption measurements were performed using the x-ray beam monochromatized by a Si(311) double crystal monochromator. The monochromator crystal temperature was kept controlled to avoid any thermal drift. For the temperature dependent measurements, the LCMO samples were mounted in a two stage closed cycle He cryostat. A reference sample (MnO_2 powder) was mounted beneath the LMCO samples to have correct energy calibration at each temperature. The temperature was monitored with an accuracy of $\pm 1\text{K}$. Fluorescence yield (FY) was recorded using 13 Ge element solid state detector system with an energy resolution of 170 eV at the Mn K-edge. Several scans were collected at each temperature to ensure high signal to noise ratio. The EXAFS analysis were performed as reported earlier (Lanzara et al, 1998).

3. Results and Discussion

Fig. 1 shows the normalized Mn K-edge x-ray absorption near edge spectra of LCMO system measured in the ferromagnetic metallic phase (at 30K) and in the insulating phase, above the CMR transition (at 250K). We observe an energy shift (ΔE_s) of about 0.4 eV towards lower energy while going from metallic to the insulating phase. In addition, we can see a clear change in the pre-peak region (see the inset) showing a sharper edge in the metallic phase while broader doublet structure in the insulating phase. We observe a decrease of the transition intensity from the 1s level to the lowest unoccupied 3d states (peak P_1) while going from the metallic to the insulating phase. This is accompanied by an increase of the absorption for transition to the higher unoccupied 3d states (peak P_2) lying at ~ 1.5 eV above the lowest unoccupied 3d states.

Fig.2. shows temperature dependence of the intensities of the peaks P_1 (panel a) and P_2 (panel b). The intensities of the two peaks show clear but opposite change across the CMR transition. The difference between the two intensities, representing the relative variation of the peak intensities, is

reported in Fig. 2(c). The variation across the metal insulator crossover is evident in the absorption difference.

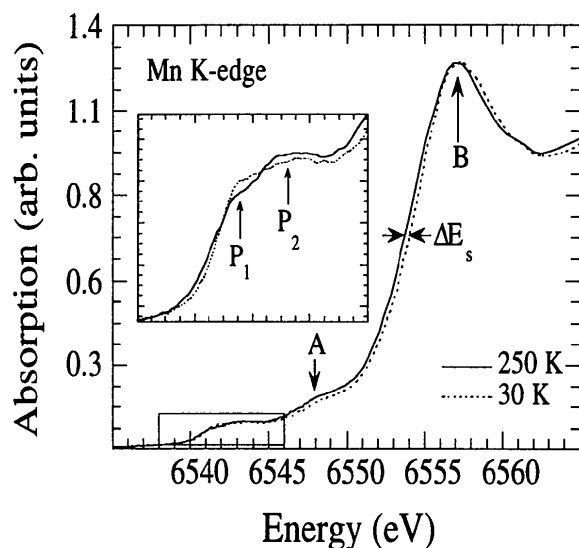


Figure 1
Normalized Mn K-edge XANES spectra of $\text{La}_{0.75}\text{Ca}_{0.25}\text{MnO}_3$ measured at 250 K (solid line) and 30 K (dotted line). The pre-edge region, corresponding to P_1 and P_2 peaks has been magnified in the inset.

Fig. 3(a) shows the temperature evolution of the energy shift of the main absorption jump (ΔE_s) as indicated in Fig. 1. The energy shift decreases with the temperature and it shows a broad transition, from 150 to 250K, when the system goes from the metallic to the insulating state. In the Mn K-edge spectrum, the main peak represents multiple scattering of the photoelectrons with the surrounding O atoms. Thus the energy shift of the main peak ΔE_s is related to the variation of the average Mn-O bondlengths. In fact, the variation of the energy shift is consistent with the EXAFS measurements as the ΔE_s decreases from 150 to 250K correlated with the elongation of Mn-O bondlengths across the metal-insulator transition.

We have already shown quantitative measurement of the Mn-O bondlengths (Lanzara et al, 1998). The temperature dependence of the probability of Mn-O bondlengths extracted from the analysis of the EXAFS spectra in Fig. 3 (panel b) and average Mn-O distance (panel c) (Lanzara et al, 1998) is compared with the energy shift of the Mn K-edge (panel b) and shown in Fig. 3

The relative probability of the Mn-O bonds allowed us to find quantitative polaronic distortions in the system. In the metallic phase ($T < T_C$), local distribution of the Mn-O bonds is a two peak function with 4 small bonds of $\sim 1.92 \pm 0.01 \text{ \AA}$ and 2 long bonds of $\sim 2.01 \pm 0.01 \text{ \AA}$ related to a small Jahn-Teller like distortion. On the other hand, in the insulating phase ($T > T_C$) the system shows higher local disorder with 4 short bonds of $\sim 1.92 \pm 0.01 \text{ \AA}$, 1 long bond of $\sim 2.01 \pm 0.01 \text{ \AA}$ and 1 longer bond of ($\sim 2.13 \pm 0.01 \text{ \AA}$). This is due to two kind of different octahedral distortions in the insulating phase. Thus the elongation of the Mn-O bondlengths across the CMR transition is due to stabilization of the small polarons with large Jahn-Teller distortion of the MnO_6 octahedra.

Coming back to the pre-peak, the electronic properties in the Ca doped $\text{La}_{1-x}\text{Ca}_x\text{MnO}_3$ are mainly controlled by the electrons in the Mn 3d orbitals. The mean number of these

electronically active electrons per Mn site is $(4-x)$. Out of these, three electrons go into the t_{2g} core states and the remaining $(1-x)$ electrons go into e_g orbitals. Thus, the lowest energy transition is due to a direct transition from $1s$ to $3d e_g (3d_{x^2-y^2})$ orbitals from the initial state $1s^2 t_{2g}^3 e_g^{1-x}$ to the final state $1s^1 t_{2g}^3 e_g^{1-x+1}$ in the presence of small octahedral distortions in the metallic state. In fact with the small MnO_6 distortions there is a small Jahn-Teller splitting between the e_g orbitals, i.e., $e_{g1} (3d_{z^2-r^2})$ and $e_{g2} (3d_{x^2-y^2})$. Above the CMR transition the system goes into stronger MnO_6 distortions increasing the Jahn-Teller splitting. The large distortions push the e_{g1} orbitals towards lower energy while the e_{g2} orbitals are pushed towards higher energy. Therefore the lowest energy core transition in the distorted Mn octahedra, with formal Mn^{3+} valence, goes from the initial state $1s^2 t_{2g}^3 e_{g1}^1 e_{g2}^0$ to the final state $1s^1 t_{2g}^3 e_{g1}^1 e_{g2}^1$. Thus the large Jahn-Teller splitting is responsible for the transfer of spectral weight of the P_1 peak to higher energy overlapping the peak P_2 .

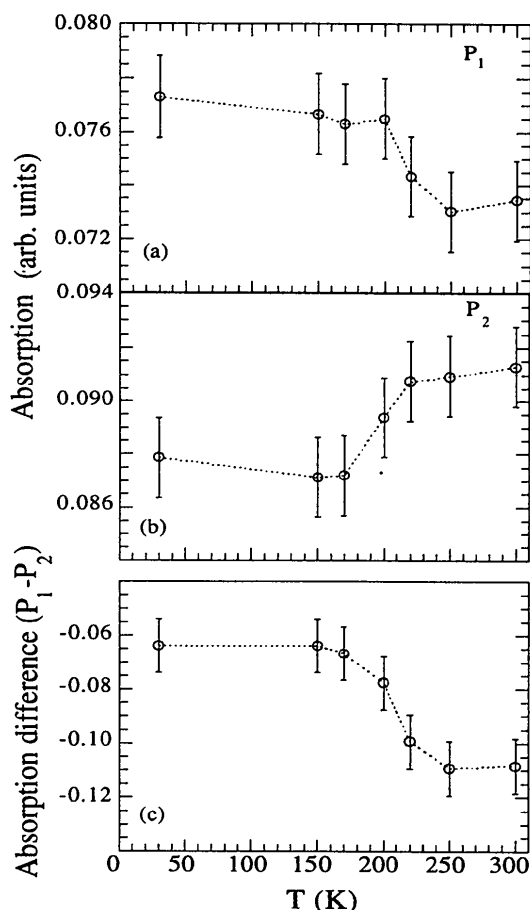


Figure 2
Temperature dependence of the intensity of P_1 (panel a) and P_2 (panel b). The difference of the P_1 and P_2 intensity is shown in panel c. The error bars represent *average uncertainty* due to normalization of different scans.

In conclusion, we have made high resolution Mn K-edge XANES measurements on the LCMO system. We have shown that the pre-peak intensity probes the Jahn-Teller splitting of e_g orbitals and follows the CMR transition. Thus the

combination of XANES and EXAFS made us to conclude that the metal to insulator transition in the CMR materials is characterized by a spatial crossover of the polaronic charges.

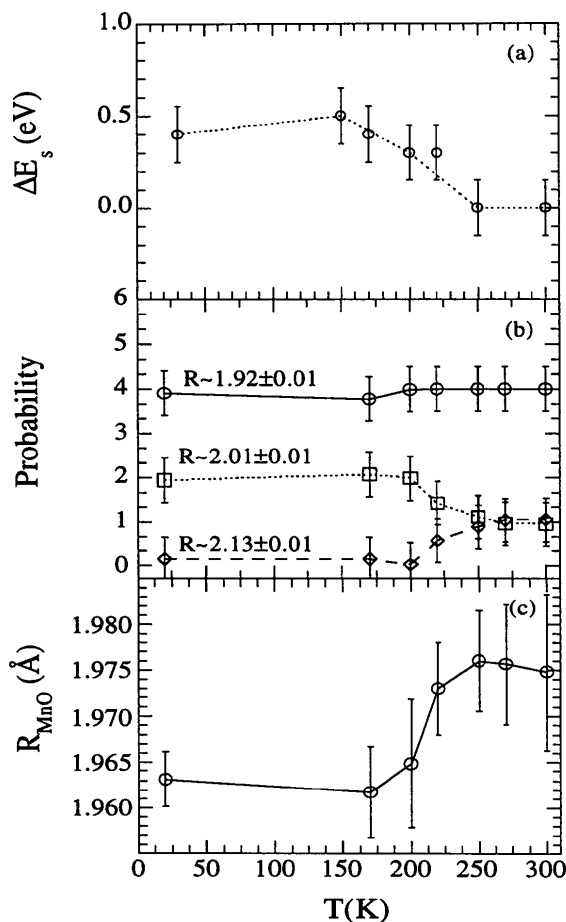


Figure 3
Temperature dependence of: (a) the energy shift of the Mn K-edge, corresponding to the maximum in the derivative spectra; (b) probability of Mn-O bondlengths; (c) average Mn-O distance.

We are happy to acknowledge the beamline staff for their help and cooperation during the experimental run. Thanks are due to S.W.Cheong for providing high quality samples and useful discussions. The work is partially supported by Istituto Nazionale di Fisica della Materia (INFM), Istituto Nazionale di Fisica Nucleare (INFN) and Consiglio Nazionale delle Ricerche (CNR).

References

- Rao, C.N.R., Mahesh, R., Raychaudhury, A.K., & Mahendiran, R. (1998). *J. Phys. Chem Solids* **59**, 487. and references therein.
 Schiffer, P., Ramirez, A. P., Bao, W., Cheong, S-W. (1995). *Phys. Rev. Lett.* **75**, 3336.
 Bishop, A.R., & Röder, H., (1997). *Current Opinion Solid State Mater. Sci.* **2**, 244.
 Millis, A.J. (1998) *Nature* **392**, 147 and references therein.
 Zhao Guo-Meng, Conder, K., Keller, H., & Muller, K. A. (1996). *Nature* **381**, 676.
 Goodenough, J.B. & Zhou, J.S. (1997) *Nature* **386**, 229. and references therein.

- Radaelli, P.G., Cox, D. E., Marezio, M., Cheong, S-W., Schiffer, P.E., & Ramirez, A.P. (1996); *Phy. Rev. Lett.* **75**, 4488; *Phys. Rev. B* **54**, 8992.
 Egami, T., Louca, Despina, McQueeney, R. J., (1997). *J. Superconductivity* **10**, 323.
 Billinge, S.J.L., Di Francesco, R.G., Kwei, G.H., Neumeier, J.J., & Thompson, D. (1996). *Phys. Rev. Lett.* **77**, 715.
 De Teresa, J.M., Ibarra, M.R., Algarabel, P.A., Ritter, C., Marquina, C.J., Blasco, Garcia, J., del Moral, A. & Arnold, Z. (1997) *Nature* **386**, 256.
 Tyson, T. A., Mustre de Leon, J., Conradson, S.D., Bishop, A.R., Neumeier, J.J., Röder, H., and Zang, Jun. (1996). *Phys. Rev. B* **53**, 13958.
 Booth, C.H., Bridges, F., Snyder G.J., & Geballe, T.H. (1996). *Phys. Rev. B* **54**, 15606.
 Lanzara, A., Saini, N.L., Brunelli, M., Natali, F., Bianconi, A., Radaelli, P.G., & Cheong, S.-W., (1998). *Phys. Rev. Lett.* **81**, 878. and references therein.

(Received 10 August 1998; accepted 11 December 1998)